Gait Phase Detection Based on LSTM-CRF for Stair Ambulation

Haochen Wei, Raymond Kai-yu Tong, Michael Yu Wang, *Fellow, IEEE*, and Chao Chen

***Abstract*—It is essential to accurately identify gait phases when active exoskeleton devices assist with the lower limbs. This work focuses on IMU-based phase detection for stair ambulation. In order to enhance the detection sensitivity of phase transition, this work utilises the LSTM-CRF hybrid model. Four IMU sensors attached to the thighs and shanks on both legs were utilised to collect data during trials on ten healthy subjects for stair ascent and descent. The network's performance is evaluated by F1-score, recall (true positive rate), and precision, which are 96.3% on average with a standard deviation (std) of 1.9%, 96.6% on average with an std of 1.6%, and 95.9% on average with an std of 2.7%, respectively.**

***Index Terms*—Deep learning methods, gait phase detection, IMU, prosthetics and exoskeletons, stair ambulation.**

I. Introduction

ALMOST one billion people worldwide suffer from certain types of disabilities, such as muscle weakness, partial or complete paralysis and loss of lower extremity assistance [1]. Furthermore, the global aging population has grown rapidly, with the study indicating that around 12% of the total population is aged 60 or over, and this proportion will continue to rise [2]. Consequently, it is urgently needed to study partially assistive exoskeletons for the benefit of elderly and disabled persons [3], [4].

Compared to fully mobilising exoskeletons designed for people who completely lose control of their legs, partial assist exoskeletons are generally lighter and primarily designed for less severe users [5]. Nevertheless, it is also challenging because the device must synchronously detect the user's intent and support the users instead of hindering them. To date, more research focuses solely on a single type of movement to identify the different phases of the gait cycle, especially level walking. Furthermore, the models they built are usually based on regular walking patterns in the laboratory environment. However, the situation outside the laboratory is more complex. Various sensors and algorithms have been studied in this field to improve the performance of gait phase detection (GDP).

The use of force platforms to evaluate foot placement, and 3D motion capture devices to determine the spatial and temporal characteristics of the limbs are the gold standard for gait analysis [6], [7]. However, they are confined to indoor environments. When considering real-life scenario using, it is preferable to use wearable sensors to measure the movement such as electromyography (EMG) [8], [9], inertial measurement unit (IMU) [10], [11], [12], and force sensor [13], [14]. EMG sensors can predict the intent of the user well before the actual movement takes place. However, many studies have shown that EMG signals are more likely to be disturbed [15]. Furthermore, EMG settings are more complex and require specialised knowledge to carry and calibrate. With respect to pressure measurements, several researchers opt for foot switches and FSRs to capture the ground contact information [16], [17]. However, compared to force platforms, the mechanical failure of these sensors commonly occurs, and the durability of analog output signals is low [18]. IMUs are cheaper and more portable than other wearable sensors [19]. In addition, many studies have shown that IMU data can be used to detect walking phases reliably [20].

A large number of different signal processing algorithms for GPD have been developed, and they could generally be categorised into two types: rule-based threshold algorithms and machine learning-based algorithms. Due to the quick processing time, rule-based threshold techniques have been used in the past [18], [21]. Despite being simple to implement, their efficacy depends on how thoroughly each phase is described, which causes a certain lack of adaptability [22]. The use of machine learning techniques in gait phase-detection systems has increased over the past ten years as it has become the norm for data processing in most other technical domains. Recently, fuzzy logic models, support vector machines [10], artificial neural networks [23], [24], hidden Markov models [25], [26] have been studied. S'anchez et al.'s study [27] contrasted the effectiveness of an HMM model algorithm with a threshold-based approach. As a result, four phases of level walking can be detected by HMM with greater precision and timing. Furthermore, RNN (like LSTM) is superior to HMM techniques in time series modelling, according to a study by Khalifa et al. [28]. The LSTM model performs better while processing lengthy data sequences because of the forget gates. Inspired by the concept of LSTM-CRF [29], we combined the two classifiers to better

Manuscript received 26 March 2023; accepted 28 July 2023. Date of publication 9 August 2023; date of current version 15 August 2023. This letter was recommended for publication by Associate Editor John-John Cabibihan and Editor Pietro Valdastri upon evaluation of the reviewers' comments. *(Corresponding author: Chao Chen.)*

This work involved human subjects or animals in its research. Approval of all ethical and experimental procedures and protocols was granted by Monash University Human Research Ethics Committee under Application No. 17072, and performed in line with the Functional Validation of Knee Brace through Treadmill Testing.

Haochen Wei, Michael Yu Wang, and Chao Chen are with the Faculty of Engineering, Monash University, Clayton, VIC 3800, Australia (e-mail: haochen.wei@monash.edu; Michael.Y.Wang@monash.edu; chao.chen@monash.edu).

Raymond Kai-yu Tong is with the Department of Biomedical Engineering, The Chinese University of Hong Kong, Hong Kong 999077, China (e-mail: kytong@cuhk.edu.hk).

Digital Object Identifier 10.1109/LRA.2023.3303787

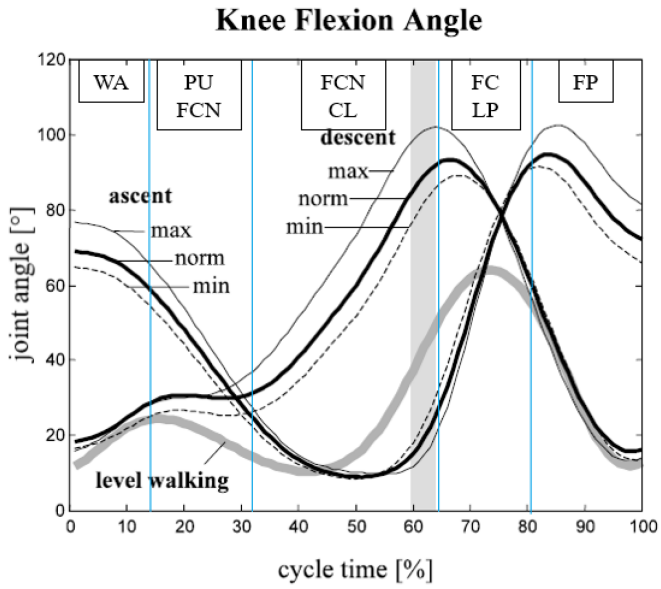

Fig. 1. Average knee flexion angle of one gait cycle of stair ascent and descent [31]. The gait cycle initiates with the foot contact, and the presence of a vertical grey bar denotes variations of foot-off instants, effectively dividing the complete stride into two distinct phases: stance and swing. The blue vertical lines are the transitions between different gait phases.

handle time-series modelling while allowing independent output labels to be associated.

Although GPD has been commonly studied, very few studies focus on stair ambulation. Based on the existing literature [30], [31], the most common way to partition the stair walking gait cycle is the five-phase method, which separates the stance phase into 3 subphases and the swing phase into 2 subphases as shown in Fig. 1. As our project focuses on the knee exoskeleton, this five-phase can well reflect the knee joint flexion angle changing nodes. Meanwhile, this gait cycle partitioning method has generalisability, since the diversity of gait patterns among different subjects is more reflected in the range of joint movement angles, but the angle variation trend is similar. Because the kinematics information was collected from healthy subjects [31], this study also conducted experiments among healthy subjects. The main contributions of this study can be summarised as follows.

- We developed an LSTM-CRF model to detect the gait phase during stair ambulance through inertial measurement units signals. The LSTM component is designed to model long-range dependencies in the input sequence, while the CRF component models dependencies between neighbouring labels in the output sequence, making the model robust to noise.
- More gait phases were able to be detected by the proposed model during stair ambulation. The model could identify Weight Acceptance (WA), Pull-Up (PU), Forward Continuance (FCN), Foot Clearance (FC), and Foot Placement (FP) phases for upstairs; Weight Acceptance (WA), Forward Continuance (FCN), Controlled Lowering (CL), Leg Pull-Through (LP), and Foot Placement (FP) for downstairs.

Algorithm 1: Spike Removal.

procedure SpikeRemovalIMU raw data, n_1, n_2
  errorIndices $\leftarrow$ empty list
  derivative $\leftarrow$ computeDerivative(data)
  for i **in** 1 **to** length(derivative) **do**
    if $|\text{derivative}[i] - \text{derivative}[i-1]| > n_1$ or $|\text{derivative}[i]| > n_2$ **then**
      $\text{data}[i] \leftarrow (\text{data}[i-1] + \text{data}[i+1])/2$
      errorIndices.append(i)
  return data, errorIndices

- Experiments were conducted to confirm that the LSTM-CRF model achieves good accuracy and is more stable than other prediction models when detecting different phases.

The remainder of this letter is organised as follows. Section II presents the implementation details of the proposed LSTM-CRF model. Section III presents the experiments to validate the proposed method and analyse their results. Finally, Sections IV and V provides a more thorough discussion of the proposed method and summarises this work.

II. Methodology

An overview of the proposed GPD system is presented in Fig. 2. It contains three stages, from signal acquisition to the prediction of gait phases. First, the signal preprocessing stage includes filtering and signal smoothing. Second, the data labelling stage uses multiple sensor signals and the rule-based method to label each phase. Finally, the LSTM-CRF model is trained and tested by the labelled dataset.

A. Data Labelling

A series of rule-based algorithms would process the raw data transmitted by the Raspberry Pi to the computer to align the IMU data with the target phases. Firstly, all variable values from IMUs and footswitches are separated and pre-processed. We smoothen the data and remove erroneous spikes. The angles are reproduced between $-180°$ and $180°$. Then the rule-based function takes an input array of data, along with two threshold values (n1 and n2). It calculates the derivative of the data and examines each derivative value. If the gradient between the current and previous value exceeds the threshold n1, or if the current derivative value exceeds the threshold n2, the corresponding data value is considered a candidate for spike removal. The function would replace each identified spike value with the midpoint between the previous and next valid data points and store the modified value's index. Finally, the function outputs the error-reduced data array and the list of indices where changes occurred.

As spikes are significantly less likely in footswitch data, a less aggressive approach can be taken. By utilizing a moving average, spikes can be mitigated, with minimal interference to the rest of the values. Based on the existing literature [1, 2], the most common way to partition the stair walking gait cycle is the five-phase method, which separates the stance phase into 3 subphases

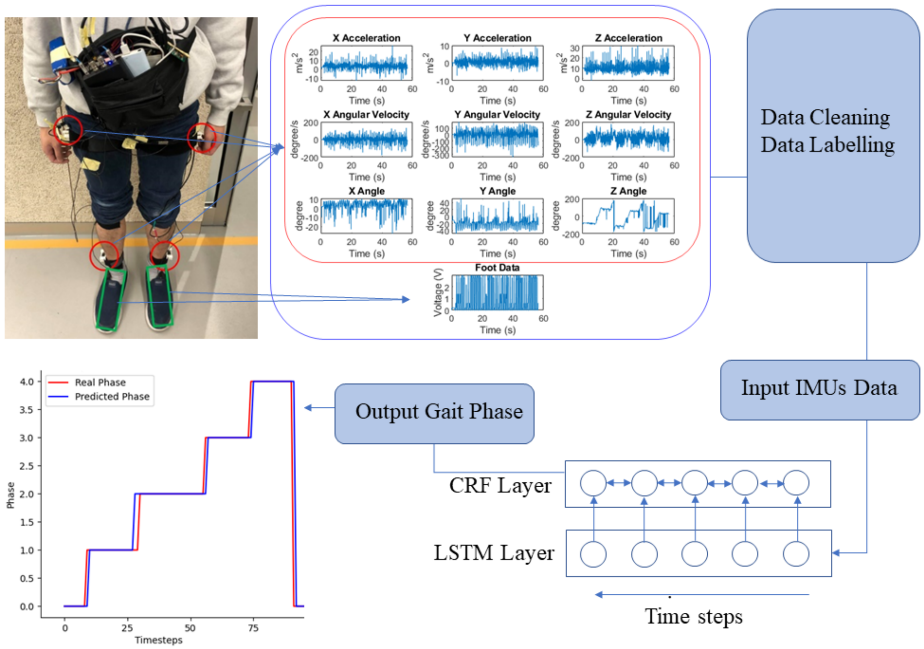

Fig. 2. Overview of the GPD system. The data collection system consists of four IMUs and two insole footswitches, which are located in red and green frames. The raw data will be cleaned and labelled into five stair ascent and five stair descent phases. Then, the IMU data is input to the LSTM-CRF model and outputs the phase prediction.

TABLE I
PARTICIPANTS PROFILES

Age	24.89 (4.19) [20,34]
Height (cm)	173.11 (9.18) [158,185]
Weight (kg)	68.78 (14.06) [48,90]
Average Cadence of Stair Ascent (step/s)	0.85 (0.1) [0.67,1.03]
Average Cadence of Stair Descent (step/s)	0.91 (0.12) [0.70,1.13]

The numbers represent the mean (standard deviation) [range] of the variables.

and the swing phase into 2 subphases. Table I summarizes the detailed partitioning for both up and down stair ambulation as well as the starting point of each phase when applying the rule-based algorithm.

After data smoothing, the IMU data will be labelled with different phases by certain rule-based thresholds based on footswitch data. These rules are according to the definitions and descriptions from previous studies [30], [31], and the videos from our experiments. Firstly, the footswitch data is tagged with non-zero and zero values, indicating the foot is on or off the ground. In this project, we take the right leg as the leading leg. And the details of determining each phase are listed below.

- The first instant of right foot-on is the starting point of WA for upstairs and downstairs. During this phase, this body shifts the weight from the contralateral leg to the ipsilateral leg.
- The WA phases are ended by the PU (upstairs) and FCN (downstairs) phases start. These two phases occur when the left foot is taking off. And the body is at the single-limb support stage.
- To determine the FCN (upstairs) and CL (downstairs), we use the IMU pitch angle. For upstairs, we obtain the instant where the right and left thighs are side by side. The absolute difference between the two pitch thigh angles must be less than a threshold (4). For downstairs, we locate the starting instant of CL by the instant where the right and left shanks are side by side. This determination gives us stable and accurate separation, which satisfies the percentage of each phase.
- Then, the gait cycle will enter the swing phase. The FC (upstairs) and LP (downstairs) are captured when the right foot leaves the ground.
- The determination of FP phases for upstairs and downstairs is as same as FCN (upstairs) and CL (downstairs) because they are both during the swing phase, and the situation is similar. And a full gait cycle ends by the WA phase starts.

B. LSTM-CRF Model Design

It is known that the RNN-based algorithm is advantageous in dealing with time-series data. Hence, we first select the LSTM model to predict the phase. Furthermore, we add the CRF layer to the LSTM model to increase the robustness due to its capability of capturing the dependencies between neighbouring label outputs. The LSTM-CRF model is built in Keras deep learning framework. The detailed architecture is shown in Fig. 3 and explained below.

The input signals come from 4 IMUs with 36 features after the data labelling process stated in the A section. The features from one IMU sensor, which comprises the acceleration signal,

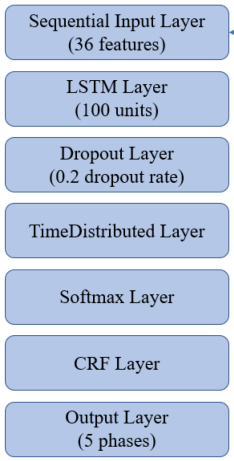

Number	IMU Feature
1	X Acceleration (m/s²)
2	Y Acceleration (m/s²)
3	Z Acceleration (m/s²)
4	X Angular Velocity (degree/s)
5	Y Angular Velocity (degree/s)
6	Z Angular Velocity (degree/s)
7	X Roll (degree)
8	Y Pitch (degree)
9	Z Yaw (degree)

Fig. 3. LSTM-CRF model architecture and the input features.

angular velocity signal, and angles from three axes, are listed in Fig. 3. Within the current range of training data, more feature inputs can better help the LSTM capture valid information for more accurate predictions.

Then the input data is transferred to the LSTM architecture with the LSTM (100 units), dropout, and TimeDistributed layer. The LSTM unit has four major components: the input gate, the forget gate, the output gate, and the memory unit. To allow the model to learn more complex patterns and capture more detailed dependencies in the input sequences while not increasing the model's computational complexity and memory requirements much, we chose 100 LSTM units with the ReLU activation function. Then to prevent the overfitting issue, the dropout layer is added, which randomly makes some values of neurons zero with a probability specified by the dropout rate. The dropout rate of 0.2 is a default value in machine learning, so we first choose this value and find it optimal for this study. Further, the TimeDistributed layer will process the data. Compared to the Dense layer, the TimeDistributed layer could help the model effectively process the temporal information in sequential data, capturing dependencies and patterns at each time step. After the model learns a new set of weights and biases, the Softmax activation layer is applied to normalise the predictions and obtain the five gait phase classification probabilities.

We add a CRF classifier layer in addition to using Softmax as the activation function for the output nodes. A CRF layer has a state transition matrix as a characteristic. With such a layer, we can efficiently use past and future labels to predict the current label. It can help when the input values become irregular, and the network can still make reasonable predictions based on previous outputs. The detailed expression is shown below.

Let y be a labelled tag sequence and x an input sequence of signals. We can compute the conditional probability for CRF as the following equation.

$$P(y \mid x) = \frac{\exp(\text{Score}(x, y))}{\sum_{y'} \exp\left(\text{Score}\left(x, y'\right)\right)} \tag{1}$$

Where log potentials are defined to determine the score value as follows.

$$Score(x, y) = \sum_i \log\psi_i(x, y) \tag{2}$$

In the LSTM-CRF network, there are two kinds of potentials: emission (E) and transition (T). The hidden state of the LSTM at timestep i serves as the source of the emission potential for the phase at index i. A $|T| \times |T|$ matrix $\boldsymbol{P}$, where T is the phase set, contains the transition scores. In the implementation, $\mathbf{P}_{j,k}$ stands for the transitioning score from phase tag k to phase tag j. So:

$$\begin{aligned} Score(x, y) &= \sum_i \log\psi_E(y_i \to x_i) + log\psi_T(y_{i-1} \to y_i) \\ &= \sum_i h_i[y_i] + P_{y_i, y_{i-1}} \end{aligned} \tag{3}$$

We tweaked the hyperparameters to obtain a better performance which was evaluated by the metrics outlined in the next section and finally chose to use ADAM optimiser, 8 batch size, and 100 epochs for the model. ADAM is an optimisation algorithm that combines the benefits of both AdaGrad and RMSProp. It can dynamically adjust the learning rate for each parameter during training and incorporate momentum to speed up convergence by utilising the exponentially decaying average of past gradients. By handling sparse gradients effectively and enabling smoother optimisation, the ADAM optimiser works well for this study.

C. Evaluation Metrics

The model accuracy performance was evaluated with recall (TPR), precision (PPV) and F1-score, which are commonly used metrics that evaluate the performance of classification models in machine learning. Recall measures the proportion of correct predictions out of the total number of actual labels, which indicates the sensitivity of the model. Precision measures the proportion of correct predictions out of the total number of predictions of one label, which indicates the precision of the model. And F1-score is a weighted harmonic mean of TPR and PPV, which is a good metric to evaluate the overall accuracy of the classification model. Mathematically, they can be defined as:

$$TPR = \frac{TP}{TP + FN} \tag{4}$$

$$PPV = \frac{TP}{TP + FP} \tag{5}$$

$$F1 = 2 \times \frac{TPR \times PPV}{TPR + PPV} \tag{6}$$

True positive (TP) is defined as correct detection within five timesteps when the actual transition happened in this work. False positive (FP) is defined as false detection that the actual transition did not happen within five timesteps. False negative (FN) is defined as the actual transition that happened but is not detected within five timesteps.

TABLE II
LSTM-CRF PERFORMANCE

Locomotion Mode	Precision	Recall	F1-score
Stair Ascent	0.953 (1.9%)	0.948 (1.7%)	0.95 (1.2%)
Stair Descent	0.959 (0.6%)	0.966 (0.8%)	0.963 (0.6%)

The numbers represent the mean (standard deviation) of the variables.

III. EXPERIMENT AND RESULTS

A. Experiment Setup

As illustrated in Fig. 2, the participants were instructed to wear two insole footswitches (B&L Engineering, USA), four IMU sensors, and a waist bag carrying additional electronic equipment (battery, Raspberry Pi, signal amplifier) at specific positions. Two IMU sensors were mounted to record the motion of the shanks, and two other IMU sensors were mounted to record the motion of the thighs. The digital low-pass filter in the Digital Motion Processor could handle the high-frequency signal noise from the accelerometer and gyroscope. The two footswitches were strategically placed on the user's shoe insoles with adhesive tape. Each footswitch comprises four switches: the heel switch produces a low voltage; the toe switch produces a high voltage; and the other two switches, located at the first and fifth metatarsals, produce two voltages that range between the levels of the heel and toe. The Raspberry Pi serves as the central hub for all the linked devices, and the virtual network connection sends 100 Hz signals to the computer.

The participants were advised to climb stairs at their preferred speed with 59 steps. Since this study focuses on normal gait detection, only step-over-step gaits were collected, while stumbling and level walking steps were removed from the database. The experiment had a total of 10 participants (7 male and 3 female). Table I summarises the participants' information.

This project (ID:17072) is considered by the Monash University Human Research Ethics Committee. It meets the requirements of the National Statement on Ethical Conduct in Human Research and has been granted approval.

B. Network Performance

The default setting is 5-fold cross-validation, with data distribution as 80% training and 20% testing. Furthermore, we analysed and compared the proposed method in different locomotion modes, subjects, and phases with other literature models.

1) Comparison With Different Locomotion Modes: There are two locomotion modes which are stair ascent and stair descent. From Table II we can see the LSTM-CRF model achieved 0.959, 0.966, 0.963 for the precision, recall, and F1-score of downstairs. And 0.953, 0.948, 0.95 for upstairs. The overall detection accuracy for two phases, which are the swing and stance phases, is 96%. And our proposed five-phase detection model accuracy could achieve 95%, which is satisfactory. Overall, the LSTM-CRF model exhibits good robustness in all modes of motion.

TABLE III
COMPARISON OF THE DETECTING MULTIPLE PHASES CAPABILITY

Algorithm		Phase					std
		HS	FF	HO	SW		
FMS-Net [32] (Level Walking)	Precision	0.738	0.945	0.982	0.992		11.9%
	Recall	0.56	0.983	0.97	0.984		20.9%
	F1-score	0.637	0.964	0.976	0.988		16.9%
		HS	FF	HO	SW		
LSTM [32] (Level Walking)	Precision		0.89	0.946	0.983		4.7%
	Recall		0.979	0.939	0.972		2.1%
	F1-score		0.933	0.943	0.978		2.4%
		WA	FCN	CL	LP	FP	
LSTM (Stair Walking)	Precision	0.89	0.904	0.974	0.903	0.964	3.9%
	Recall	0.888	0.923	0.962	0.939	0.974	3.4%
	F1-score	0.889	0.913	0.968	0.921	0.969	3.5%
		WA	FCN	CL	LP	FP	
LSTM-CRF (Stair Walking)	Precision	0.912	0.964	0.979	0.969	0.975	2.7%
	Recall	0.954	0.957	0.992	0.973	0.957	1.6%
	F1-score	0.932	0.96	0.986	0.971	0.966	1.9%

HS is heel strike; FF is foot flat; HO is heel off; SW is swing.

2) Comparisons Among Subjects: The variability in biological and kinematic features between subjects is relatively high, which could be found in several existing studies. We could also find the average cadence differences from the table of volunteers' profiles. Hence, the capability of the detection model to deal with data from unknown subjects is critical to be validated. K-fold cross-validation is a common method to estimate the skill of a machine learning model on unseen data. After regrouping, the testing data would always contain kinematics characteristics from subjects that haven't been trained. In Table II, we listed the standard deviation (std) between different groups' testing results. For stair ascent, the std is at an average of 0.016. And it's even lower than 0.01 when going downstairs, which shows that our proposed LSTM-CRF model is relatively robust for new subjects' data.

3) Comparison With Other Methods: Because there is a relatively small amount of studies focusing on gait phase detection of the staircase; moreover, the detecting system setups and the model outputs are various. Therefore, we have yet to find an existing work detecting similar multiple phases for stair ambulation like ours. Zhen et al. [32] used three acceleration sensors and various machine-learning models to detect multiple phases for level walking on the treadmill. Table III lists the three-metric accuracy of different methods for individual phases during gait cycles. Although the phases differ between level and stair walking, some partitioning methods are similar. We also reproduced an LSTM-only model to run our dataset for more statistical analysis and comparison. The T-test was conducted. The confidence intervals of standard deviation do not overlap, and the P-value is 0.003, less than 0.05. It suggests that we have enough evidence to reject the null hypothesis and conclude that there is a significant difference between the two groups of results. The confidence interval of precisions overlaps and the T-statistic is negative 1.228 indicating there may not be a significant difference between the two groups, but the mean of LSTM precision is slightly lower than the mean of LSTM-CRF. This is reasonable because the LSTM-CRF model, rather than

enhancing the overall precision significantly, is more likely to improve the lowest accuracy and keep the prediction at a relatively stable high accuracy. These comparison results show that our LSTM-CRF model is more reliable for detecting multiple phases with relatively high and stable accuracy.

IV. Discussion

From the results in the tables above, the LSTM-CRF model shows superior performance, especially in stability among phase transitions or subject changes. That is because LSTM-CRF is a powerful machine-learning model that combines the strengths of LSTM and CRF models. It is particularly effective for sequential labelling tasks, where the CRF layer helps capture the dependencies between neighbouring labels that are impossible with LSTM-only models. LSTM-CRF can make more accurate predictions than simple RNN models, as the CRF layer adds a regularisation term that encourages the model to predict sequences of labels that are more likely to occur. Additionally, LSTM-CRF can handle rare events better than RNN models, as the CRF layer can model the overall distribution of labels in the training data and use this information to make better predictions. The output of an LSTM-CRF model is more interpretable than the output of an RNN model, as it produces a sequence of labels that represents the most likely labelling for the input sequence, making it a powerful and effective tool for sequential labelling tasks. These characteristics make the LSTM-CRF model promising and reliable in the active exoskeleton application.

Although the model shows superiority, there is still room for improvement. First is the manual labelling of gait phases due to the unavailability of an existing database for training the model. Since we only based on the footswitch and IMU information, slight accuracy differences could appear. Future studies would benefit from a larger, standardised database for training the model. We may also consider introducing vision sensors to help with labelling. Besides, this study currently only focuses on the healthy young adult group. Getting certain patients with trouble walking involved is necessary to verify the model. Furthermore, due to the algorithm's complexity, adding a CRF layer to the LSTM network can cause more computation time. The time error is around 55 ms for the LSTM-CRF model, which still needs further optimisation to reduce the computation time and ensure faster prediction performance to apply it to the real-time operating exoskeleton. Moreover, while our initial application focused on a real-life environment, future enhancements should aim for better prediction accuracy with fewer sensors. Reducing the sensor requirements would improve the practicality and feasibility of implementing the gait phase detection system in real-life scenarios. Lastly, the experiments of this study were only conducted in one building. To ensure robustness, more different staircases will be selected to collect data.

V. Conclusion

In this study, we developed an LSTM-CRF model to detect five gait sub-phases during stair ambulation. The proposed method shows stable and high accuracy among different sub-phases and subjects. The proposed method was validated on data from blueten healthy subjects and improved the prediction performance of gait phase detection during stair ambulance from other machine learning methods. Applying the LSTM-CRF gait phase detection algorithm in an active lower-limb exoskeleton is without the scope of this study. In the future, we will validate the effectiveness of the LSTM-CRF model in a rehabilitative lower-extremity exoskeleton system in real-time operation. Additionally, we will apply this model to more motion modes in uncontrolled environments.

References

[1] B. Kalita, J. Narayan, and S. K. Dwivedy, "Development of active lower limb robotic-based orthosis and exoskeleton devices: a systematic review," *Int. J. Social Robot.*, vol. 13, pp. 1–19, 2020.

[2] WHO, "Ageing and health," *World Health Org.*, 2022. Accessed: Feb. 2023. https://www.who.int/news-room/fact-sheets/detail/ageing-and-health

[3] H. Kawamoto and Y. Sankai, "Power assist method based on phase sequence and muscle force condition for HAL," *Adv. Robot.*, vol. 19, no. 7, pp. 717–734, 2005.

[4] D. Novak and R. Riener, "A survey of sensor fusion methods in wearable robotics," *Robot. Auton. Syst.*, vol. 73, pp. 155–170, 2015.

[5] R. Baud, A. R. Manzoori, A. Ijspeert, and M. Bouri, "Review of control strategies for lower-limb exoskeletons to assist gait," *J. NeuroEng. Rehabil.*, vol. 18, no. 1, pp. 1–34, 2021.

[6] C. M. O'Connor, S. K. Thorpe, M. J. O'Malley, and C. L. Vaughan, "Automatic detection of gait events using kinematic data," *Gait Posture*, vol. 25, no. 3, pp. 469–474, 2007.

[7] R. J. Foster, A. R. De Asha, N. D. Reeves, C. N. Maganaris, and J. G. Buckley, "Stair-specific algorithms for identification of touch-down and foot-off when descending or ascending a non-instrumented staircase," *Gait Posture*, vol. 39, no. 2, pp. 816–821, 2014.

[8] C. D. Joshi, U. Lahiri, and N. V. Thakor, "Classification of gait phases from lower limb EMG: Application to exoskeleton orthosis," in *Proc. IEEE Point-of-Care Healthcare Technol.*, 2013, pp. 228–231.

[9] A. Khan and E. Biddiss, "Musical stairs: A motivational therapy tool for children with disabilities featuring automated detection of stair-climbing gait events via inertial sensors," *Med. Eng. Phys.*, vol. 40, pp. 95–102, 2017, doi: 10.1016/j.medengphy.2016.12.009.

[10] Z. Zhou, X. Liu, Y. Jiang, J. Mai, and Q. Wang, "Real-time onboard SVM-based human locomotion recognition for a bionic knee exoskeleton on different terrains," in *Proc. Wearable Robot. Assoc. Conf.*, 2019, pp. 34–39.

[11] T. Lee, I. Kim, and S.-H. Lee, "Estimation of the continuous walking angle of knee and ankle (talocrural joint, subtalar joint) of a lower-limb exoskeleton robot using a neural network," *Sensors*, vol. 21, no. 8, 2021, Art. no. 2807.

[12] L. Wang, Y. Sun, Q. Li, T. Liu, and J. Yi, "Two shank-mounted IMUs-Based gait analysis and classification for neurological disease patients," *IEEE Robot. Automat. Lett.*, vol. 5, no. 2, pp. 1970–1976, Apr. 2020, doi: 10.1109/LRA.2020.2970656.

[13] B. T. Smith, D. J. Coiro, R. Finson, R. R. Betz, and J. McCarthy, "Evaluation of force-sensing resistors for gait event detection to trigger electrical stimulation to improve walking in the child with cerebral palsy," *IEEE Trans. Neural Syst. Rehabil. Eng.*, vol. 10, no. 1, pp. 22–29, Mar. 2002.

[14] P. Catalfamo, D. Moser, S. Ghoussayni, and D. Ewins, "Detection of gait events using an F-scan in-shoe pressure measurement system," *Gait Posture*, vol. 28, no. 3, pp. 420–426, 2008, doi: 10.1016/j.gaitpost.2008.01.019.

[15] F. Labarrière et al., "Machine learning approaches for activity recognition and/or activity prediction in locomotion assistive devices—A systematic review," *Sensors*, vol. 20, no. 21, 2020, Art. no. 6345.

[16] V. Agostini, G. Balestra, and M. Knaflitz, "Segmentation and classification of gait cycles," *IEEE Trans. Neural Syst. Rehabil. Eng.*, vol. 22, no. 5, pp. 946–952, Sep. 2014.

[17] J. Yang et al., "Machine learning based adaptive gait phase estimation using inertial measurement sensors," in *Proc. Front. Biomed. Devices*, 2019, Paper V001T09A010.

[18] F. Maqbool, M. A. B.M. I. Husman, A. Awad, N. Abouhossein Iqbal, and A. A. Dehghani-Sanij, "A real-time gait event detection for lower limb prosthesis control and evaluation," *IEEE Trans. Neural Syst. Rehabil. Eng.*, vol. 25, no. 9, pp. 1500–1509, Sep. 2017.

[19] M. Hanlon and R. Anderson, "Real-time gait event detection using wearable sensors," *Gait Posture*, vol. 30, no. 4, pp. 523–527, 2009.
[20] J. Taborri, E. Palermo, S. Rossi, and P. Cappa, "Gait partitioning methods: A systematic review," *Sensors (Basel)*, vol. 16, no. 1, 2016, Art. no. 66, doi: 10.3390/s16010066.
[21] N. C. Bejarano, E. Ambrosini, A. Pedrocchi, G. Ferrigno, M. Monticone, and S. Ferrante, "A novel adaptive, real-time algorithm to detect gait events from wearable sensors," *IEEE Trans. Neural Syst. Rehabil. Eng.*, vol. 23, no. 3, pp. 413–422, May 2015, doi: 10.1109/TNSRE.2014.2337914.
[22] M. Stanley, "Gait phase detection of stair ambulation using inertial measurement of lower limb," Ph.D. dissertation, Dept. Mech. Aerosp. Eng., Monash Univ., Melbourne, VIC, Australia, 2021.
[23] K. Bhakta, J. Camargo, L. Donovan, K. Herrin, and A. Young, "Machine learning model comparisons of user independent and dependent intent recognition systems for powered prostheses," *IEEE Robot. Automat. Lett.*, vol. 5, no. 4, pp. 5393–5400, Oct. 2020, doi: 10.1109/LRA.2020.3007480.
[24] D.-H. Moon, D. Kim, and Y.-D. Hong, "Development of a single leg knee exoskeleton and sensing knee center of rotation change for intention detection," *Sensors*, vol. 19, no. 18, 2019, Art. no. 3960.
[25] J. Bae and M. Tomizuka, "Gait phase analysis based on a hidden Markov model," *Mechatronics*, vol. 21, no. 6, pp. 961–970, 2011.
[26] A. Mannini, V. Genovese, and A. M. Sabatini, "Online decoding of hidden Markov models for gait event detection using foot-mounted gyroscopes," *IEEE J. Biomed. Health Inform.*, vol. 18, no. 4, pp. 1122–1130, Jul. 2014.
[27] M. D. S'anchez Manchola, M. J. P. Bernal, M. Munera, and C. A. Cifuentes, "Gait phase detection for lower-limb exoskeletons using foot motion data from a single inertial measurement unit in hemiparetic individuals," *Sensors*, vol. 19, no. 13, 2019, Art. no. 2988.
[28] Y. Khalifa, D. Mandic, and E. Sejdi'c, "A review of hidden Markov models and recurrent neural networks for event detection and localization in biomedical signals," *Inf. Fusion*, vol. 69, pp. 52–72, 2021.
[29] Z. Huang, W. Xu, and K. Yu, "Bidirectional LSTM-CRF models for sequence tagging," 2015, *arXiv:1508.01991*.
[30] B. J. McFadyen and D. A. Winter, "An integrated biomechanical analysis of normal stair ascent and descent," *J. Biomech.*, vol. 21, no. 9, pp. 733–744, 1988.
[31] R. Riener, M. Rabuffetti, and C. Frigo, "Stair ascent and descent at different inclinations," *Gait Posture*, vol. 15, no. 1, pp. 32–44, 2002, doi: 10.1016/s0966-6362(01)00162-x.
[32] T. Zhen, L. Yan, and J.-l. Kong, "An acceleration based fusion of multiple spatiotemporal networks for gait phase detection," *Int. J. Environ. Res. Public Health*, vol. 17, no. 16, 2020, Art. no. 5633.